

# Study of Asphaltene Precipitation during CO<sub>2</sub> Injection into Oil Reservoirs in the Presence of Iron Oxide Nanoparticles by Interfacial Tension and Bond Number Measurements

Rafat Parsaei,\* Yousef Kazemzadeh, and Masoud Riazi

Cite This: <https://dx.doi.org/10.1021/acsomega.9b04090>

Read Online

ACCESS |

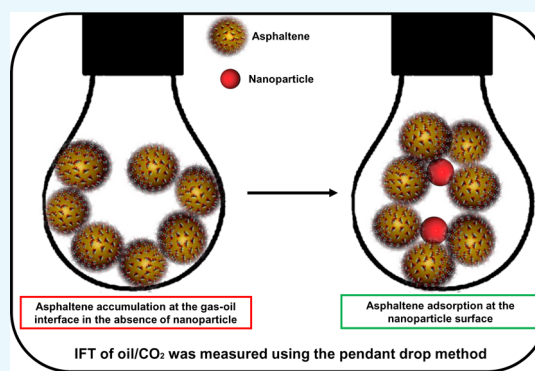


Metrics &amp; More



Article Recommendations

**ABSTRACT:** CO<sub>2</sub> injection is one of the most frequently used enhanced oil recovery methods; however, it causes asphaltene precipitation in porous media and wellbore and wellhead facilities. Carbon dioxide saturated with nanoparticles can be used to enhance oil recovery with lower asphaltene precipitation issues. In this study, the vanishing interfacial tension technique was used to investigate the possibility of diminishing asphaltene precipitation by nanoparticles. The interfacial tension (IFT) of synthetic oil/carbon dioxide was measured using the pendant drop method. The results illustrated that, for synthetic oil samples containing asphaltene, the IFT data versus pressure decrease linearly with two different slopes at low- and high-pressure ranges. At high pressures, the slope of the plot is lower than the one in the low-pressure range. The addition of iron oxide nanoparticles to the oil solution reduces the interfacial tension at higher pressures with a steeper slope, showing that nanoparticles can decrease asphaltene precipitation. The plot of Bond number versus pressure also confirmed the impact of nanoparticles on reducing asphaltene precipitation. In terms of the temperature effect, the presence of nanoparticles at 50 °C resulted in a 16.34% reduction in asphaltene precipitation and a 19.65% reduction at 70 °C. The minimum miscibility pressure changed from 10.17 to 30.96 MPa at 70 °C; however, in the presence of nanoparticles, it reduced from 10.06 to 16.56. Therefore, the technique introduced in this study could be applied to avoid the problems associated with altering the gas injection mode from miscible to immiscible.



## 1. INTRODUCTION

Production from oil reservoirs with a high percentage of asphaltene is associated with many problems,<sup>1,2</sup> including the reduction of the reservoir uptake, serious problems in the wellbore and processing facilities and, therefore, a significant increase in the cost of extraction and exploitation.<sup>3–5</sup> Gas injection, changes in pH, joining of the oil flows with different compositions, incompatible organic chemicals, and shear stress are among the most important factors that cause asphaltene precipitation during oil production and transmission.<sup>2,6–8</sup> Therefore, finding a solution to reduce or prevent asphaltene precipitation is necessary.<sup>9</sup>

Dissolution by various solvents (e.g., toluene and xylene) has been considered as one of the mostly used methods for eliminating asphaltene precipitation.<sup>9,10</sup> The proposed methods are generally limited to certain technical conditions, and the utilized chemicals are hazardous to the environment. For this reason, the use of modern technologies such as nanoparticles has gained increasing interest since they are more effective and economical.<sup>3,10,11</sup> Due to their very high surface-to-volume ratio, high degree of suspension, and high adsorption strength, nanoparticles are very capable of

suspending asphaltene particles and preventing asphaltene precipitation. Also, nanoparticles, which are typically in the form of metal particles or metal oxide, are able to remove the precipitated asphaltene through their heat catalyst characteristics.<sup>6,11,12</sup> Therefore, investigating the performance of metal oxide nanoparticles in preventing asphaltene precipitation during CO<sub>2</sub> injection for recovery of heavy oil has been the focus of research in recent years.<sup>6,7,11,13</sup> Nassar et al. conducted several experiments to investigate the effect of various operating parameters and types of nanoparticles on the asphaltene precipitation reduction for oil samples with high asphaltene content.<sup>14–18</sup> Comparing nanoparticles including oxides of nickel, cobalt, and iron, they concluded that their performance in terms of adsorption and catalytic ability is as follows: NiO > CO<sub>3</sub>O<sub>4</sub> > Fe<sub>3</sub>O<sub>4</sub>.<sup>16</sup> They also found that

Received: December 1, 2019

Accepted: March 24, 2020

microsized particles exhibit better catalytic ability, but the nanoparticles can adsorb more. Asphaltene adsorption on the surface of the nanoparticles is spontaneous and exothermic in nature.<sup>16,17</sup> They found that the amount of asphaltene adsorption is proportional to the contact time of nanoparticles and crude oil. Nevertheless, their results showed that most of the adsorption occurs at the early time of contact, and later on, the amount of adsorption is negligible. Also, the greater the initial saturation of asphaltene, the higher the adsorption rate. Moreover, they concluded that, with the temperature rise, the rate of asphaltene adsorption is reduced. In terms of other available molecules, it was found that, as the amount of normal heptane increases, the asphaltene adsorption rate increases as well.<sup>14–18</sup> Babamahmoudi and Riahi<sup>19</sup> and Shokrlu and Babadagli<sup>20–22</sup> compared the performance of nanoparticles and microsized particles of pure nickel and found that the catalytic performance and the adsorption capacity of nanoparticles are better, both of which improve oil mobility and avoid asphaltene precipitation. Ogolo et al. identified several mechanisms through which nanoparticles can improve the oil recovery, including rock wettability alteration, interfacial tension (IFT) reduction, oil viscosity reduction, mobility ratio decrease, and permeability changes.<sup>23</sup> Nassar in another study showed that, as the asphaltene molecular weight decreases, the adsorption rate of iron oxide nanoparticles improves.<sup>24</sup> Abu Tarboush in a study on the asphaltene adsorption by nickel oxide nanoparticles indicated that this type of nanoparticle has a high adsorption capacity.<sup>25</sup> The injection of nanoparticles is one of the most attractive enhanced oil recovery methods due to the different mechanisms addressed above.<sup>2,19</sup> The asphaltene precipitation reduction is one of the most important roles of injecting nanoparticles.<sup>26</sup>

Among different methods for detecting the onset and intensity of asphaltene precipitation, the disappearance of the interfacial tension method is a new method.<sup>11,12,27</sup> In this method, the interfacial tension of oil and gas is plotted against pressure. This gives a linear plot whose slope changes suddenly when the asphaltene starts to precipitate. The amount of slope change could also be considered as the intensity of precipitation.<sup>6,11</sup> This method requires a small amount of sample to perform the test.<sup>28</sup> The method for the disappearance of interface tension is rapid, repeatable, and is also very useful for calculation of the optimal conditions for injecting the mixture of gases into oil reservoirs.<sup>6,9,28</sup> In this study, this method was used to address the impact of the nanoparticles on the onset point and intensity of asphaltene precipitation. The plot of Bond number versus pressure is another tool that was previously used by the authors of this study to detect the onset of asphaltene precipitation.<sup>6,7</sup> This method was again applied here to detect the conditions under which asphaltene starts to precipitate in the presence of nanoparticles. The Bond number is defined as the ratio of gravity force to the capillary force exerted on a pendant drop and is given by the following equation<sup>29–31</sup>

$$\text{bond number} = \frac{b^2 g \Delta \rho}{\gamma} \quad (1)$$

where  $\gamma$  is the IFT,  $b$  is the radius of curvature at the apex of the drop,  $g$  is the gravitational acceleration, and  $\Delta \rho$  is the density difference between the two fluids. A high value of Bond number means that the shape of the pendant drop is more

affected by the gravity force, and it is elongated toward the vertical direction. On the other hand, if the relative strength of the capillary force is higher than the gravity force, which is the case for low values of the Bond number, the shape of the drop becomes more spherical.

All definitions of miscibility require the absence of an interface between the injected gas and the crude oil at reservoir conditions at the point of miscibility. This means that the interfacial tension between two immiscible fluids must continuously diminish as they approach miscibility and become zero at the point of miscibility.<sup>32,33</sup> In the vanishing interfacial tension (VIT) technique, the miscibility conditions of pressure and composition are determined as the pressure at which the interfacial tension is zero. However, it is impossible to measure interfacial tension when it becomes zero. Hence, the VIT technique relies on measuring gas–oil interfacial tension to a value as low as the experimental accuracy allows and then extrapolating the data to zero interfacial tension. Thus, the VIT technique requires accurate measurement of gas–oil interfacial tension at reservoir conditions.<sup>34</sup> In those reservoirs where asphaltene precipitation occurs due to changes in the oil composition, the minimum miscibility pressure (MMP) increases. This means that a miscible gas injection process may convert to an immiscible process. For the first time, in this study, we estimated the amount of change in the MMP following asphaltene precipitation. Also, an attempt was made to investigate the impact of iron oxide nanoparticles on asphaltene stability and hence the miscibility conditions during a CO<sub>2</sub> injection process.

## 2. EXPERIMENTAL SECTION

**2.1. Materials.** Synthetic oil solutions were used that contained toluene, normal heptane, and asphaltene (extracted from the crude oil taken from an oil field located in the south of Iran).

In general, to detect the possibility of thermodynamic instability of asphaltene, there are four methods based on the practical correlations. These four methods include De Boer charts, Stankevich methods, colloidal instability index, and asphaltene stability index.<sup>1</sup> In the colloidal stability index method, the CII index is determined using eq 2:<sup>12</sup>

$$\text{CII} = \frac{x_{\text{Saturate}} + x_{\text{Asphaltene}}}{x_{\text{Aromatic}} + x_{\text{Resin}}} \quad (2)$$

The value of this index is directly related to the stability of asphaltene. If CII is less than 0.7, the asphaltene precipitation is unlikely. When this index falls between 0.7 and 0.9, there is a possibility of precipitation; if this index becomes more than 0.9, the likelihood of precipitation of asphaltenes increases.<sup>1</sup> The SARA analysis of the utilized oil is shown in Table 1. Using these data, the CII of the oil was estimated to be 0.83, meaning that there is a chance of asphaltene to precipitate for

**Table 1. SARA Analysis Performed on the Crude Oil Used for Asphaltene Extraction**

type	wt %
saturates	34.28
aromatics	37.72
resins	16.97
asphaltenes	11.03

this oil type. The effect of CO<sub>2</sub> on CII will be discussed in the subsequent section.

Asphaltene was extracted from the crude oil using the ASTM standard (D2007-80).<sup>7,10,35</sup> Then 5 wt % asphaltene was dissolved in a mixture of toluene and normal heptane (40 vol % *n*-heptane and 60 vol % toluene) to make the asphaltenic oil samples. CO<sub>2</sub> gas with a purity of 99.99% was used for surface tension measurements.

The utilized nanoparticles were provided by US Research Nanomaterials Inc. The surface and physical properties of the nanoparticle and its scanning electron microscopy (SEM) image are presented in Table 2 and Figure 1, respectively.

**Table 2. Surface Properties and Appearance of Iron Oxide (Fe<sub>3</sub>O<sub>4</sub>) Nanoparticles**

purity (%)	APS (nm)	SSA (BET m <sup>2</sup> /g)	color	morphology	bulk density (g/cm <sup>3</sup> )	true density (g/cm <sup>3</sup> )
99	20–30	81.98	brown	spherical	0.85	4.80–5.10

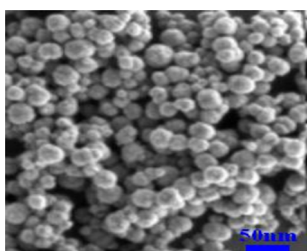


**Figure 1.** SEM of Fe<sub>3</sub>O<sub>4</sub> NPs provided by the US Research Nanomaterials Inc.

To prepare oil solutions containing nanoparticles, 1 wt % iron oxide nanoparticles were added to the oil sample, and the mixture was shaken by a centrifuge at an angular velocity of 5000 rpm at room temperature. The mixture was then shaken

at 200 rpm in an incubator for 24 h. Finally, it was sonicated in a water bath at 25 °C for 2 h to stabilize the suspension.<sup>6</sup>

**2.2. IFT Measurement Tests.** The impact of nanoparticles on the onset condition of asphaltene precipitation was studied by measuring the gas–oil interfacial tension at reservoir conditions using the pendant drop method. To calculate the interfacial tension at a particular temperature and pressure, the densities of the two fluids at the pertinent temperature and pressure were required. Therefore, the liquid density was measured using an Anton Paar density meter (DMA-HPM) with high accuracy at different pressures and temperatures. Gas density, at different pressures and temperatures, was taken from a reliable reference.<sup>36</sup> Carbon dioxide gas has a relatively low critical pressure (7.39 MPa). At critical pressure, the carbon dioxide density rises suddenly and behaves similarly to the liquids. Since carbon dioxide density is considered as an input in calculations of IFT, the effect of such a phase change is inherently included in the calculation of interfacial tension.

The experimental setup for interfacial tension measurement is shown in Figure 2. The setup includes a visual high-pressure chamber made of Hastelloy, equipped with two glass windows placed in front and at the back of the chamber. The high-pressure chamber also consists of a capillary tube that is located on the top of it through which oil is injected into the chamber using a high-pressure pump, and a pendant drop is formed at the tip of the capillary tube.

The system is placed in a controlled thermal chamber. A high-resolution camera is placed in front of the chamber and a light source on the other side for providing enough light to take a picture from the pendant drop. The camera is connected to a computer by which the interfacial tension of oil and gas is calculated using the drop shape analysis software.

Before starting an experiment, the whole apparatus is cleaned with toluene and acetone followed by rinsing with water. Then the two fluid tanks, namely, the drop-phase tank (DT) and the bulk-phase tank (BT), are filled with the drop fluid (here, oil) and the bulk fluid (here, gas), respectively. Next, the temperatures of the visual chamber, the bulk-fluid

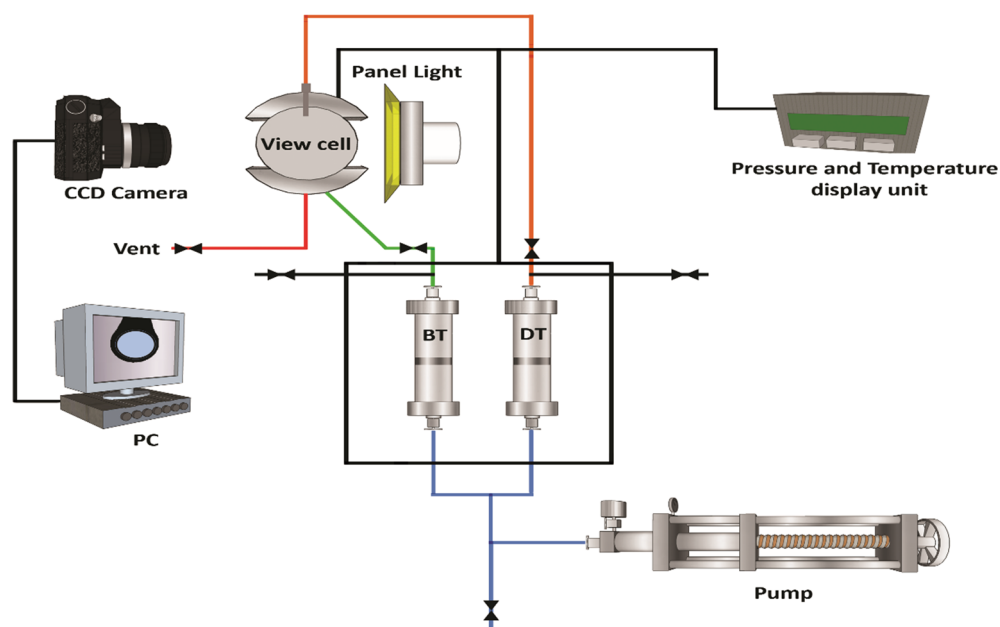


**Figure 2.** Schematic illustration of the experimental setup.

tank, and the drop-fluid tank are set at the desired values. The gas is then injected into the visual high-pressure chamber that was set at the reservoir temperature earlier. The gas injection process will continue until reaching the desired pressure. Enough time is given to the whole system to reach a perfect balance (i.e., the condition that the temperature and pressure of the visual chamber remain stable). To form the drop phase, oil is then injected slowly by opening the valve on the top of the chamber. After obtaining a stable drop, the interfacial tension is calculated by the software based on the shape of the pendant drop. Figure 3 shows a sample of images illustrating the change in the shape of the oil droplet, surrounded by CO<sub>2</sub>, under different visual cell pressures at 50 °C.

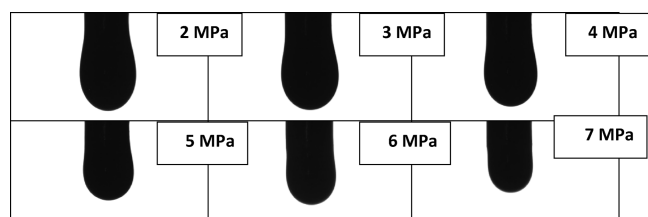


**Figure 3.** Shape of an oil drop in the presence of CO<sub>2</sub> under different cell pressures at 50 °C.

### 3. RESULTS AND DISCUSSION

The effect of nanoparticles on asphaltene precipitation was studied by preparing a number of synthetic oil solutions and measuring their surface tension in the presence of carbon dioxide at different temperatures and pressures. The reproducibility of the experimental results was checked by repeating each test at least four times, and the average value was considered as the IFT at a particular pressure and temperature. The amount of standard deviation for the IFT and the Bond number data at each temperature and pressure condition were about 0.1 mN/m and 0.01, respectively.

**3.1. Interfacial Tension of Asphaltenic Solutions at 50 °C.** Two types of oil samples were prepared with a similar composition (i.e., 40 vol % *n*-heptane and 60 vol % toluene), one containing 1 wt % iron oxide nanoparticles and one without nanoparticles. The IFTs of these two samples and CO<sub>2</sub> were measured at 50 °C and different pressures as shown in Figure 4.

Figure 4 demonstrates that IFT decreases linearly with increasing pressure for both solutions, at the low-pressure

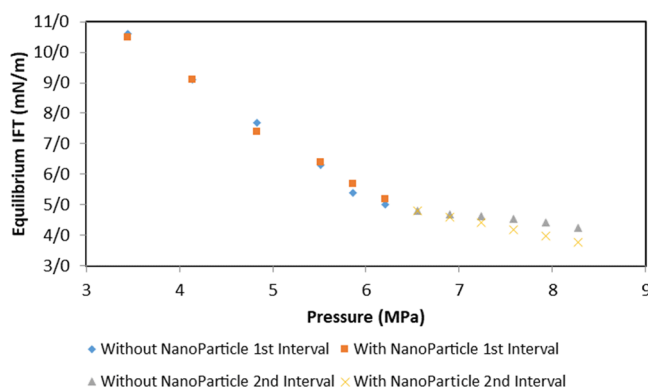


**Figure 4.** IFT versus pressure for oil solution–CO<sub>2</sub> system at 50 °C.

range (i.e., 3 to 6 MPa). Also, the two plots overlap in this pressure range. At high pressures (more than 3 MPa), asphaltene precipitation causes the slope of the diagram to decrease to 14% of its initial slope. However, in the oil solution containing iron dioxide nanoparticles, this slope reduction is smaller, i.e., 30% of the initial slope. When having nanoparticles in the oil solution, they are adsorbed by the asphaltene particles and prevent them from depositing on the interface of oil and gas. This makes asphaltene to remain in the oil bulk solution by adsorbing the large particles. If asphaltene deposits at the oil–gas interface, then the balance of intermolecular forces breaks down. Therefore, by increasing pressure, the IFT decrease is smaller. However, nanoparticles reduce the movement of the particles toward the interface by adsorbing asphaltene molecules during the solution preparation process. Therefore, the IFT reduces much more with increasing pressure compared to the solution without nanoparticles. This is because the asphaltene molecules aggregate by increasing the pressure in the solution without nanoparticles and precipitate after joining together, but the presence of nanoparticle reduces the aggregation of asphaltene particles. Despite the existence of nanoparticles in the oil bulk and the ability to adsorb large asphaltene molecules, this slope change is observed in the diagram of IFT versus pressure. As a result, nanoparticles of iron oxide cannot prevent the movement of all large molecules of asphaltene toward the interface of two fluids. In other words, these nanoparticles are not able to completely eliminate the asphaltene precipitation. The effect of CO<sub>2</sub> injection on asphaltene precipitation could also be explained using the CII index described in eq 2. CO<sub>2</sub> can be considered as a saturated hydrocarbon. Therefore, with the addition of carbon dioxide, the numerator of eq 2 increases, and so, the index rises, which means that asphaltene goes into instability. Typically, the asphaltene precipitation starts from pressures above the bubble pressure (i.e., upper asphaltene precipitation) and reaches its maximum at the bubble pressure. At lower pressures than bubble pressure (i.e., lower asphaltene precipitation), the precipitation stops. Therefore, gas injection increases precipitation. Adsorption of asphaltene by nanoparticles prevents its precipitation in a greater compression range during gas injection.<sup>37,38</sup> Table 3 shows the IFT versus pressure equations for both solutions in different intervals.

As can be seen in Table 3, for the synthetic solution that does not contain nanoparticles of iron oxide, when pressure increases, the IFT data of the two intervals decrease with two different slopes. In the first interval, the IFT reduction occurs with a steeper slope, but in the second interval, due to the asphaltene precipitation, the IFT drops with a smaller slope. The second slope is about 15% of the first slope. When 1 wt % iron oxide nanoparticles are added to the synthetic solution, the IFT in the first interval does not change so much and drops nearly with the same slope as the solution without nanoparticles. However, the IFT in the second interval of the solution containing nanoparticles drops with a steeper slope compared to the solution without nanoparticles. If the ratio of slope change in the second interval and the first interval can be assumed as the intensity of asphaltene precipitation, then by adding the nanoparticles of iron oxide to the oil sample, the intensity of asphaltene precipitation decreases. According to the VIT theory, the pressure at which the IFT of the two fluids becomes zero is considered as the minimum miscibility pressure (MMP) of the two fluids. Since the slope of the IFT diagram changes as the asphaltene starts to precipitate,



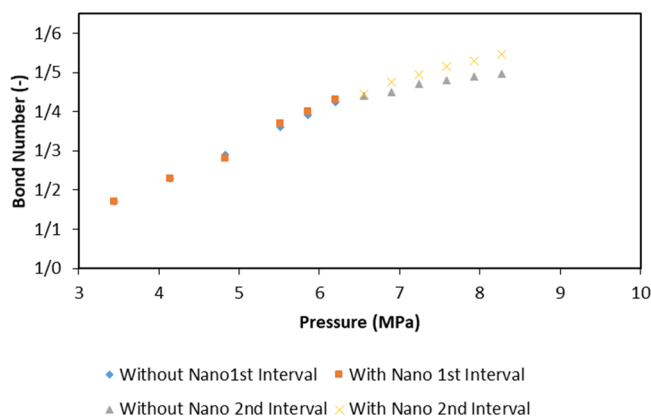
**Table 3.** IFT Versus Pressure Equations for Oil Solution–CO<sub>2</sub> System at 50 °C

oil solution type	interval	equation $P$ (MPa) IFT $\left(\frac{\text{mN}}{\text{m}}\right)$	MMP <sup>a</sup> (MPa)	the ratio of the 2nd interval slope relative to the 1st interval slope (%)
without nanoparticles	1st interval	IFT = $-2.0671P + 17.6830$	8.55	85.17
	2nd interval	IFT = $-0.3066P + 6.8295$	22.27	
with nanoparticles	1st interval	IFT = $-1.9327P + 17.045$	8.82	69.60
	2nd interval	IFT = $-0.6025P + 8.7575$	14.53	

<sup>a</sup>Minimum miscibility pressure.

two separate intervals of IFT versus pressure data are created. Each of these intervals gives its individual MMP. Therefore, the MMP of the two fluids also decreases as a result of asphaltene precipitation. The fourth column of Table 3 shows the MMP obtained from the first and second interval slopes. The results show that the presence or absence of nanoparticles in the oil solution does not affect the MMP obtained from the slope of the first interval. However, in the second interval, the presence of nanoparticles of iron oxide causes the MMP of the solution containing asphaltene to decrease to 14.53 MPa compared to 22.27 MPa in the absence of nanoparticles.

Figure 5 shows the Bond number versus pressure diagram for the two oil samples (one containing 1 wt % iron oxide

**Figure 5.** Bond number versus pressure for oil solution–CO<sub>2</sub> system at 50 °C.

nanoparticles and another without nanoparticles) in the presence of CO<sub>2</sub> at a temperature of 50 °C. It was realized that one of the methods for determining the onset of asphaltene precipitation is to plot the Bond number versus the pressure. The Bond number is the ratio of gravity force to capillary force. By increasing the pressure, the Bond number also increases. However, asphaltene precipitation causes the slope of the Bond number–pressure diagram to decrease. Therefore, similar to the IFT–pressure diagram, two different intervals are seen in the diagram of Bond number versus pressure.

As shown in Figure 5, the presence of nanoparticles in the oil samples does not change the values of the Bond number in the first interval. However, it increases the Bond number in the second interval starting from a specific pressure corresponding to the onset of asphaltene precipitation. In other words, the presence of nanoparticles in the oil solution causes the second slope of the plot of Bond number versus pressure to become steeper than the solution without nanoparticles. If the ratio of the second interval slope to the first one is taken as a criterion for the intensity of asphaltene precipitation, then because adding nanoparticles reduces the slope change of the second

interval compared to the first interval, this means that the intensity of asphaltene precipitation reduces.

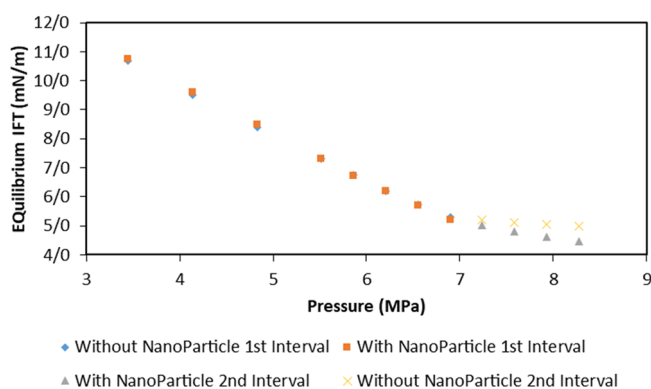
Table 4 shows the fitted equations for Bond number versus pressure data of the first and second intervals. According to

**Table 4.** Bond Number Versus Pressure Equations for Oil Solution–CO<sub>2</sub> System in at 50 °C

oil solution type	interval	equation $P$ (MPa) B. N. (–)	the ratio of the 2nd interval slope to the 1st interval slope (%)
without nanoparticles	1st interval	B.N. = $0.0933P + 0.8447$	73.42
	2nd interval	B.N. = $0.0284P + 1.2594$	
with nanoparticles	1st interval	B.N. = $0.0957P + 0.8340$	47.03
	2nd interval	B.N. = $0.0507P + 1.1237$	

Table 4, in the solution without iron oxide nanoparticles, the second slope of the Bond number versus the pressure plot is approximately 27% of the first slope, and in the solution containing 1 wt % iron oxide nanoparticles, the slope of the second interval is approximately 53% of the slope of the first interval. In other words, if we approximate the intensity of asphaltene precipitation by the ratio of slope change in the second interval to the first interval, then the intensity of asphaltene precipitation in the diagram without nanoparticles of iron oxide is close to 73%, but adding nanoparticles reduces it to 47%. In order to generalize the results, the conducted tests were repeated at 70 °C, as will be discussed in the following section.

**3.2. Effect of Iron Oxide Nanoparticle on Asphaltene Precipitation at a Temperature of 70 °C.** Figure 6 displays the IFT versus pressure plot of the two tested solutions with CO<sub>2</sub> at a temperature of 70 °C. As can be seen in this figure, at 70 °C temperature, similar to the temperature of 50 °C, two

**Figure 6.** IFT versus pressure for oil solution–CO<sub>2</sub> system at 70 °C.

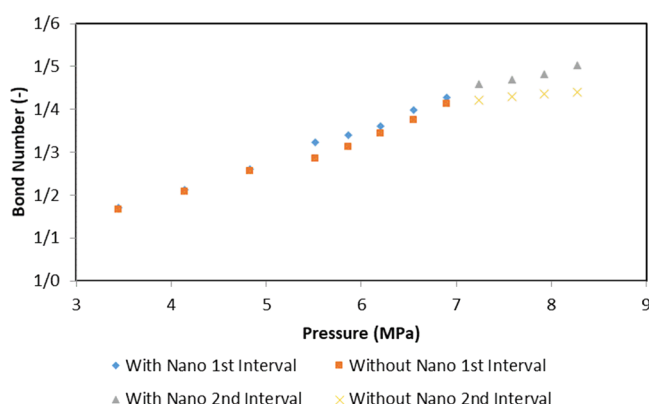
**Table 5. IFT Versus Pressure Equations for Oil Solution–CO<sub>2</sub> System at 70 °C**

oil solution type	interval	equation $P$ (MPa) IFT $\left(\frac{\text{mN}}{\text{m}}\right)$	MMP (MPa)	the ratio of the 2nd interval slope relative to the 1st interval slope (%)
without nanoparticles	1st interval	IFT = $-1.5776P + 16.0500$	10.17	86.58
	2nd interval	IFT = $-0.2117P + 6.7350$	30.96	
with nanoparticles	1st interval	IFT = $-1.6231P + 16.3120$	10.06	66.94
	2nd interval	IFT = $-0.5366P + 8.8850$	16.56	

intervals are observed for each solution. In the first interval, the values of IFT of the two solutions drop approximately with the same slope.

Table 5 shows the details of the interval slopes and values of the MMP obtained by each of the two slopes. As shown in Table 5, due to asphaltene precipitation at the interface of the two fluids in the solution without nanoparticles of iron oxide, the slope of the second intervals of the IFT versus pressure diagram is 13% of the first slope. Meanwhile, the addition of 1 wt % iron oxide nanoparticles to the solution causes the slope of the second interval to become about 33% of the first interval. This means that adding 1 wt % nanoparticles reduces the asphaltene precipitation by 20%. Comparing the MMPs corresponding to the first and second intervals in each of the solutions with and without nanoparticles, it is concluded that the ones obtained by the first slope are not so much different. Meanwhile, in the second interval, asphaltene precipitation causes the MMPs to increase up to 3 times of the ones of the first interval. The addition of nanoparticles to the solution makes the MMP obtained from the second interval to decrease to half of the case that there is no nanoparticle in the solution.

Figure 7 shows the Bond number versus pressure diagram for the two oil solutions (with and without iron oxide

**Figure 7.** Bond number versus pressure diagram for oil solution–CO<sub>2</sub> system at 70 °C.

nanoparticles) in the vicinity of CO<sub>2</sub>. As shown in Figure 7, in the first interval, the slope of the two diagrams for both solutions is approximately equal. However, in the second interval where the asphaltene precipitation occurs, the existence of nanoparticles causes an increase in the slope of the plots of Bond number versus pressure.

Table 6 displays the detail of slope change for the two tested solutions. As Table 6 shows, asphaltene precipitation in the solution without nanoparticles has led to the slope of the diagram to reduce from 0.0687 to 0.0187. However, in the presence of nanoparticles, the slope of the diagram decreases from 0.0746 to 0.0412. In other words, the slope change of the second interval is 82.78% compared to the first interval in the

**Table 6. Bond Number Versus Pressure Equations for Oil Solution–CO<sub>2</sub> System at 50 °C**

oil solution type	interval	equation $P$ (MPa) B. N. (–)	the ratio of the slope of the 2nd interval relative to the 1st interval slope (%)
without nanoparticles	1st interval	B.N. = $0.0687P + 0.9224$	82.78
	2nd interval	B.N. = $0.0187P + 1.2878$	
with nanoparticles	1st interval	B.N. = $0.0746P + 0.9064$	44.78
	2nd interval	B.N. = $0.0412P + 1.1590$	

solution without nanoparticles. This means that, with the addition of 1 wt % nanoparticles of iron oxide to the oil solution, this change reaches 44.78%.

For the case of live oil, asphaltene precipitation is closely related to the bubble pressure. Whenever the pressure gets closer to the bubble pressure, a higher amount of precipitation is observed. However, dead oil was used in this study. Thus, by increasing pressure, the solubility of the gas in the oil phase increases. The dissolution of gas in the oil phase causes asphaltene instability. Therefore, in this case, pressure changes affect asphaltene stability. Therefore, asphaltene precipitation in the present study could not be solely interpreted using the PVT data.<sup>39,40</sup>

### 3.3. Comparing the Effect of Iron Oxide Nanoparticle on Asphaltene Precipitation at 70 and 50 °C. Table 7

**Table 7. Comparison of the Slopes of the IFT Versus Pressure Diagrams at 50 and 70 °C**

temperature	oil solution type	1st interval slope	2nd interval slope	the ratio of the slope of the 2nd interval to the 1st interval (%)
50 °C	without nanoparticles	2.07	0.31	14.83
	with nanoparticles	1.93	0.60	31.17
70 °C	without nanoparticles	1.58	0.21	13.41
	with nanoparticles	1.62	0.54	33.06

shows the slopes of the IFT versus pressure diagrams for both solutions with and without iron oxide nanoparticles under CO<sub>2</sub> at two temperatures of 50 and 70 °C. According to this table, for the solution without nanoparticles at 50 °C, the slope of the first interval is 2.07 (mN/m)/MPa, which reduces to 0.31 (mN/m)/MPa at the second interval; this means that the slope reaches 14.83% of its initial value. However, at 70 °C, the second slope is 13.41% of the first slope. These results show that the intensity of asphaltene precipitation at 70 °C is slightly higher. In the case of solutions containing nanoparticles, the slopes change with less intensity at both levels of temperatures.

According to Table 7, at 50 °C, the slope of the second interval is 31.17% of the first interval, while at a temperature of 70 °C, it is 33.06%.

Table 8 compares the slopes of the Bond number versus pressure diagrams for the two solutions at two temperatures of

**Table 8. Comparison of the Slopes of the Bond Number Versus Pressure Diagrams at 50 and 70 °C**

temperature	oil solution type	1st interval slope	2nd interval slope	the ratio of the slope of the 2nd interval to the 1st interval (%)
50 °C	without nanoparticles	0.09	0.03	30.44
	with nanoparticles	0.10	0.05	52.98
70 °C	without nanoparticles	0.07	0.02	27.22
	with nanoparticles	0.07	0.04	55.23

50 and 70 °C. As can be seen in Table 8, the ratios of the slope of the second interval to the one of the first interval for the Bond number versus pressure diagram when the solution does not contain nanoparticles at temperatures of 50 °C and 70 °C are 30.44 and 27.22%, respectively. The comparison of these two numbers shows that asphaltene precipitation occurs slightly more at 70 °C. The same result is obtained from the data of Bond number as the slope ratios are 52.98 and 55.23% at temperatures of 50 and 70 °C, respectively.

#### 4. CONCLUSIONS

IFT measurement was conducted to investigate the impact of iron oxide nanoparticles on asphaltene precipitation behavior and MMP upon the CO<sub>2</sub> injection process. The following results can be drawn from the experimental results:

- The IFT data of synthetic solutions (containing toluene and normal heptane) and CO<sub>2</sub> decrease as pressure increases. When the oil solution is free of asphaltene, the IFT data drop with a constant slope as pressure increases. However, the presence of asphaltene in the solution makes the slope of the IFT versus pressure diagram to change at a specific pressure, corresponding to the onset pressure of asphaltene precipitation.
- Two intervals with two different slopes can be seen over the IFT versus pressure diagram because of precipitation of asphaltene and hence reduction of IFT. The amount of reduction of the second slope can give an estimate of the intensity of asphaltene precipitation.
- Another technique to detect the onset of asphaltene precipitation is to plot the Bond number data versus pressure. By increasing pressure, the Bond number follows an upward trend. In the solution without asphaltene, the Bond number increases with a constant slope as the pressure increases. However, when there is asphaltene in the oil solution, the slope of the diagram starts to decrease as asphaltene starts to precipitate.
- Prediction of the onset point and intensity of asphaltene precipitation through the data of Bond number versus pressure is in good agreement with the ones obtained by the plot of the IFT data versus pressure.
- It is possible to reduce asphaltene precipitation by using nanoparticles through their high adsorption ability. They keep asphaltene molecules in the bulk solution and

prevent them from the collision. The phenomenon of reducing asphaltene precipitation by nanoparticles was observed at both temperatures of 50 and 70 °C.

- Injection of CO<sub>2</sub> into the oil reservoirs causes asphaltene precipitation. This gives rise to altering the oil composition and hence the minimum miscibility pressure. The results of the current study could be utilized to prevent the problems associated with the change in the EOR process from miscible to immiscible mode.

#### AUTHOR INFORMATION

##### Corresponding Author

Rafat Parsaei — Department of Petroleum Engineering, School of Chemical and Petroleum Engineering, Shiraz University, Shiraz 71348-51154, Iran; [orcid.org/0000-0002-5803-0259](https://orcid.org/0000-0002-5803-0259); Email: [rparsaei@shirazu.ac.ir](mailto:rparsaei@shirazu.ac.ir)

##### Authors

Yousef Kazemzadeh — Department of Petroleum Engineering, School of Chemical and Petroleum Engineering, Shiraz University, Shiraz 71348-51154, Iran; [orcid.org/0000-0002-5021-1856](https://orcid.org/0000-0002-5021-1856)

Masoud Riazi — Department of Petroleum Engineering, School of Chemical and Petroleum Engineering and Enhanced Oil Recovery (EOR) Research Center, School of Chemical and Petroleum Engineering, Shiraz University, Shiraz 71348-51154, Iran; [orcid.org/0000-0003-0572-1766](https://orcid.org/0000-0003-0572-1766)

Complete contact information is available at: <https://pubs.acs.org/10.1021/acsomega.9b04090>

##### Notes

The authors declare no competing financial interest.

#### ACKNOWLEDGMENTS

The authors are grateful to Dr. Malayeri for his valuable advice. The authors would also like to thank Ms. Noorbakhsh, Mr. Zabihi, and Mr. Hasanpour for their help over the course of this study.

#### REFERENCES

- (1) Guzmán, R.; Ancheyta, J.; Trejo, F.; Rodríguez, S. Methods for determining asphaltene stability in crude oils. *Fuel* **2017**, *188*, 530–543.
- (2) Kazemzadeh, Y.; Eshraghi, S. E.; Kazemi, K.; Sourani, S.; Mehrabi, M.; Ahmadi, Y. Behavior of asphaltene adsorption onto the metal oxide nanoparticle surface and its effect on heavy oil recovery. *Ind. Eng. Chem. Res.* **2015**, *54*, 233–239.
- (3) Subramanian, S.; Buscetti, L.; Simon, S.; Sacré, M.; Sjöblom, J. Influence of Fatty-Alkylamine Amphiphile on the Asphaltene Adsorption/Deposition at the Solid/Liquid Interface under Precipitating Conditions. *Energy Fuels* **2018**, *32*, 4772–4782.
- (4) Cruz, A. A.; Amaral, M.; Santos, D.; Palma, A.; Franceschi, E.; Borges, G. R.; Coutinho, J. A. P.; Palácio, J.; Dariva, C. CO<sub>2</sub> influence on asphaltene precipitation. *J. Supercrit. Fluids* **2019**, *143*, 24–31.
- (5) Alimohammadi, S.; Zendehboudi, S.; James, L.; Amin, J. S. Investigation of Asphaltene Precipitation; an Experimental and CPA EOS Approaches. In *81st EAGE Conference and Exhibition 2019*, 2019.
- (6) Kazemzadeh, Y.; Malayeri, M. R.; Riazi, M.; Parsaei, R. Impact of Fe<sub>3</sub>O<sub>4</sub> nanoparticles on asphaltene precipitation during CO<sub>2</sub> injection. *J. Nat. Gas Sci. Eng.* **2015**, *22*, 227–234.
- (7) Kazemzadeh, Y.; Parsaei, R.; Riazi, M. Experimental study of asphaltene precipitation prediction during gas injection to oil

reservoirs by interfacial tension measurement. *Colloids Surf., A* **2015**, 466, 138–146.

(8) Zanganeh, P.; Dashti, H.; Ayatollahi, S. Comparing the effects of CH<sub>4</sub>, CO<sub>2</sub>, and N<sub>2</sub> injection on asphaltene precipitation and deposition at reservoir condition: a visual and modeling study. *Fuel* **2018**, 217, 633–641.

(9) Eshraghi, S. E.; Kazemzadeh, Y.; Etemadan, Z.; Papi, A. Detecting high-potential conditions of asphaltene precipitation in oil reservoir. *J. Dispersion Sci. Technol.* **2018**, 39, 943–951.

(10) Doryani, H.; Kazemzadeh, Y.; Parsaei, R.; Malayeri, M. R.; Riazi, M. Impact of asphaltene and normal paraffins on methane-synthetic oil interfacial tension: An experimental study. *J. Nat. Gas Sci. Eng.* **2015**, 26, 538–548.

(11) Hassanpour, S.; Malayeri, M. R.; Riazi, M. Utilization of Co<sub>3</sub>O<sub>4</sub> nanoparticles for reducing precipitation of asphaltene during CO<sub>2</sub> injection. *J. Nat. Gas Sci. Eng.* **2016**, 31, 39–47.

(12) Rezvani, H.; Kazemzadeh, Y.; Sharifi, M.; Riazi, M.; Shojaei, S. A new insight into Fe<sub>3</sub>O<sub>4</sub>-based nanocomposites for adsorption of asphaltene at the oil/water interface: An experimental interfacial study. *J. Pet. Sci. Eng.* **2019**, 177, 786–797.

(13) Doryani, H.; Malayeri, M. R.; Riazi, M. Visualization of asphaltene precipitation and deposition in a uniformly patterned glass micromodel. *Fuel* **2016**, 182, 613–622.

(14) Franco, C. A.; Nassar, N. N.; Ruiz, M. A.; Pereira-Almao, P.; Cortés, F. B. Nanoparticles for inhibition of asphaltenes damage: adsorption study and displacement test on porous media. *Energy Fuels* **2013**, 27, 2899–2907.

(15) Nassar, N. N. Asphaltene adsorption onto alumina nanoparticles: kinetics and thermodynamic studies. *Energy Fuels* **2010**, 24, 4116–4122.

(16) Nassar, N. N.; Hassan, A.; Pereira-Almao, P. Comparative oxidation of adsorbed asphaltenes onto transition metal oxide nanoparticles. *Colloids Surf., A* **2011**, 384, 145–149.

(17) Nassar, N. N.; Hassan, A.; Pereira-Almao, P. Metal oxide nanoparticles for asphaltene adsorption and oxidation. *Energy Fuels* **2011**, 25, 1017–1023.

(18) Nassar, N. N.; Hassan, A.; Pereira-Almao, P. Application of nanotechnology for heavy oil upgrading: Catalytic steam gasification/cracking of asphaltenes. *Energy Fuels* **2011**, 25, 1566–1570.

(19) Babamahmoudi, S.; Riahi, S. Application of nano particle for enhancement of foam stability in the presence of crude oil: Experimental investigation. *J. Mol. Liq.* **2018**, 499.

(20) Hamed Shokrlu, Y.; Babadagli, T. Effects of nano-sized metals on viscosity reduction of heavy oil/bitumen during thermal applications, In *Canadian Unconventional Resources and International Petroleum Conference*, Society of Petroleum Engineers: 2010.

(21) Shokrlu, Y. H.; Babadagli, T. Transportation and interaction of nano and micro size metal particles injected to improve thermal recovery of heavy-oil, In *SPE Annual Technical Conference and Exhibition*, Society of Petroleum Engineers: 2011.

(22) Shokrlu, Y. H.; Babadagli, T. Viscosity reduction of heavy oil/bitumen using micro- and nano-metal particles during aqueous and non-aqueous thermal applications. *J. Pet. Sci. Eng.* **2014**, 119, 210–220.

(23) Ogolo, N. A.; Olafuyi, O. A.; Onyekonwu, M. O. Enhanced oil recovery using nanoparticles, In *SPE Saudi Arabia section technical symposium and exhibition*, Society of Petroleum Engineers: 2012.

(24) Nassar, N. N. Iron oxide nanoadsorbents for removal of various pollutants from wastewater: an overview. *Appl. Adsorbents Water Pollut. Control* **2012**, 81–118.

(25) Abu Tarboush, B. *Adsorption and Oxidation of Asphaltenes onto in situ Prepared and Commercial Nanoparticles*. Unpublished doctoral thesis, University of Calgary, 2014.

(26) Karambeigi, M. S.; Nasiri, M.; Asl, A. H.; Emadi, M. A. Enhanced oil recovery in high temperature carbonates using microemulsions formulated with a new hydrophobic component. *J. Ind. Eng. Chem.* **2016**, 39, 136–148.

(27) Rezvani, H.; Khalilnezhad, A.; Ganji, P.; Kazemzadeh, Y. How ZrO<sub>2</sub> nanoparticles improve the oil recovery by affecting the

interfacial phenomena in the reservoir conditions? *J. Mol. Liq.* **2018**, 252, 158–168.

(28) Kazemzadeh, Y.; Sharifi, M.; Riazi, M.; Rezvani, H.; Tabaei, M. Potential effects of metal oxide/SiO<sub>2</sub> nanocomposites in EOR processes at different pressures. *Colloids Surf., A* **2018**, 559, 372–384.

(29) Lashkarbolooki, M.; Riazi, M.; Ayatollahi, S. Experimental investigation of dynamic swelling and Bond number of crude oil during carbonated water flooding; Effect of temperature and pressure. *Fuel* **2018**, 214, 135–143.

(30) Lashkarbolooki, M.; Riazi, M.; Ayatollahi, S. Effect of CO<sub>2</sub> and crude oil type on the dynamic interfacial tension of crude oil/carbonated water at different operational conditions. *J. Pet. Sci. Eng.* **2018**, 170, 576–581.

(31) Adamson, A. W.; Gast, A. P. *Physical chemistry of surfaces*. Interscience publishers New York: 1967; Vol. 150.

(32) Escrochi, M.; Mehranbod, N.; Ayatollahi, S. The gas–oil interfacial behavior during gas injection into an asphaltenic oil reservoir. *J. Chem. Eng. Data* **2013**, 58, 2513–2526.

(33) Rao, D. N.; Lee, J. I. Application of the new vanishing interfacial tension technique to evaluate miscibility conditions for the Terra Nova Offshore Project. *J. Pet. Sci. Eng.* **2002**, 35, 247–262.

(34) Gu, Y.; Hou, P.; Luo, W. Effects of four important factors on the measured minimum miscibility pressure and first-contact miscibility pressure. *J. Chem. Eng. Data* **2013**, 58, 1361–1370.

(35) Kazemzadeh, Y.; Eshraghi, S. E.; Riazi, M.; Zendehboudi, S. How do metal oxide nanoparticles influence on interfacial tension of asphaltic oil-Supercritical CO<sub>2</sub> systems? *J. Supercrit. Fluids* **2018**, 135, 1–7.

(36) Lemmon, E.; Huber, M.; McLinden, M. NIST Standard Reference Database 23, Reference Fluid Thermodynamic and Transport Properties (REFPROP), version 9.0, National Institute of Standards and Technology. *R1234yf. fld file dated December* **2010**, 22, 2010.

(37) Varamesh, A.; Hosseinpour, N. Prediction of asphaltene precipitation in reservoir model oils in the presence of Fe<sub>3</sub>O<sub>4</sub> and NiO nanoparticles by cubic plus association equation of state. *Ind. Eng. Chem. Res.* **2019**, 58, 4293–4302.

(38) Tabzar, A.; Fathinasab, M.; Salehi, A.; Bahrami, B.; Mohammadi, A. H. Multiphase flow modeling of asphaltene precipitation and deposition. *Oil Gas Sci. Technol.* **2018**, 73, 51.

(39) Fazlali, A.; Nikookar, M.; Mohammadi, A. H. Computational procedure for determination of minimum miscibility pressure of reservoir oil. *Fuel* **2013**, 106, 707–711.

(40) Shirazani, E. Z.; Behbahani, T. J. Development of minimum tie line length method for determination of minimum miscible pressure in gas injection process. *Pet. Res.* **2019**, 4, 173–180.